

New Tetrazole-based Cu(I) Homo- and Heteroleptic Complexes with Various Diphosphine Ligands: Synthesis, Characterization and Study of their Redox and Photophysical Properties

Cristina Femoni,^a Sara Muzzioli,^a Antonio Palazzi,^a Stefano Stagni,^{a*} Stefano Zacchini,^a Filippo Monti,^b Gianluca Accorsi,^b Margherita Bolognesi,^b Nicola Armaroli,^{b*} Massimiliano Massi,^c Giovanni Valenti^d, Massimo Marcaccio^d

^a*Dipartimento di Chimica Fisica ed Inorganica, Università di Bologna, Viale Risorgimento 4, I-40136 Bologna, Italy.* e-mail: stefano.stagni@unibo.it

^b*Molecular Photoscience Group, Istituto per la Sintesi Organica e la Fotoreattività, Consiglio Nazionale delle Ricerche (CNR-ISOF), Via Gobetti 101, I-40129 Bologna,* e-mail: nicola.armaroli@cnr.it

^c*Department of Chemistry, Curtin University, GPO Box U 1987, Perth, Australia, 6845.*

^d*Dipartimento di Chimica “G. Ciamician”, Università di Bologna, Via Selmi 2, I-40126 Bologna, Italy.*

SUPPORTING INFORMATION

Selected ESI-MS spectra

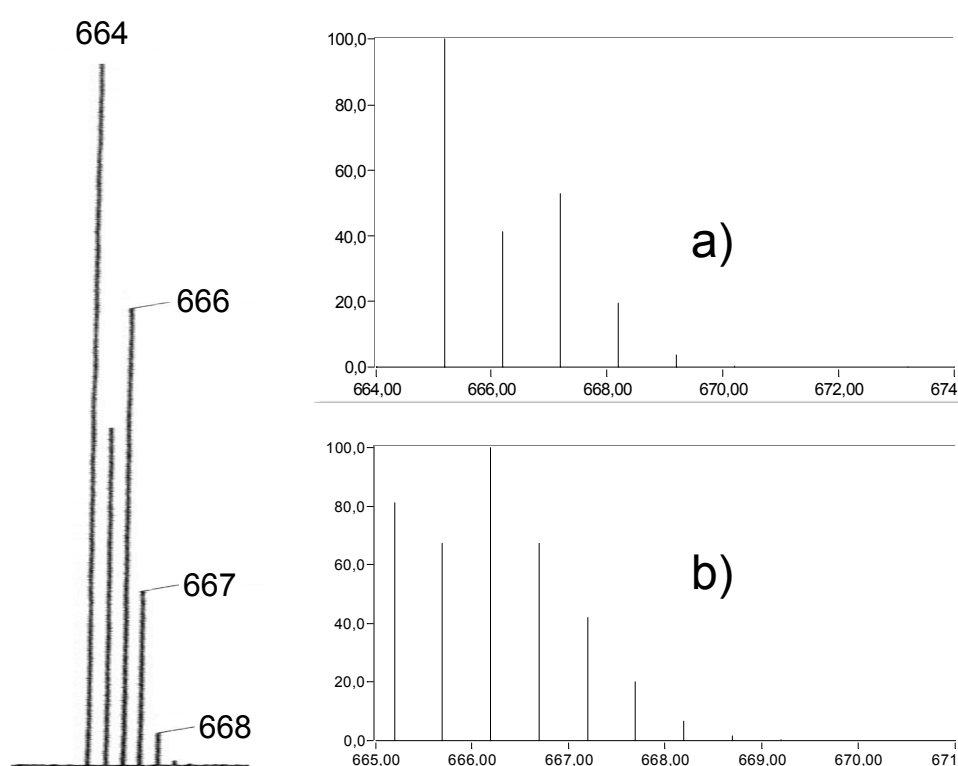
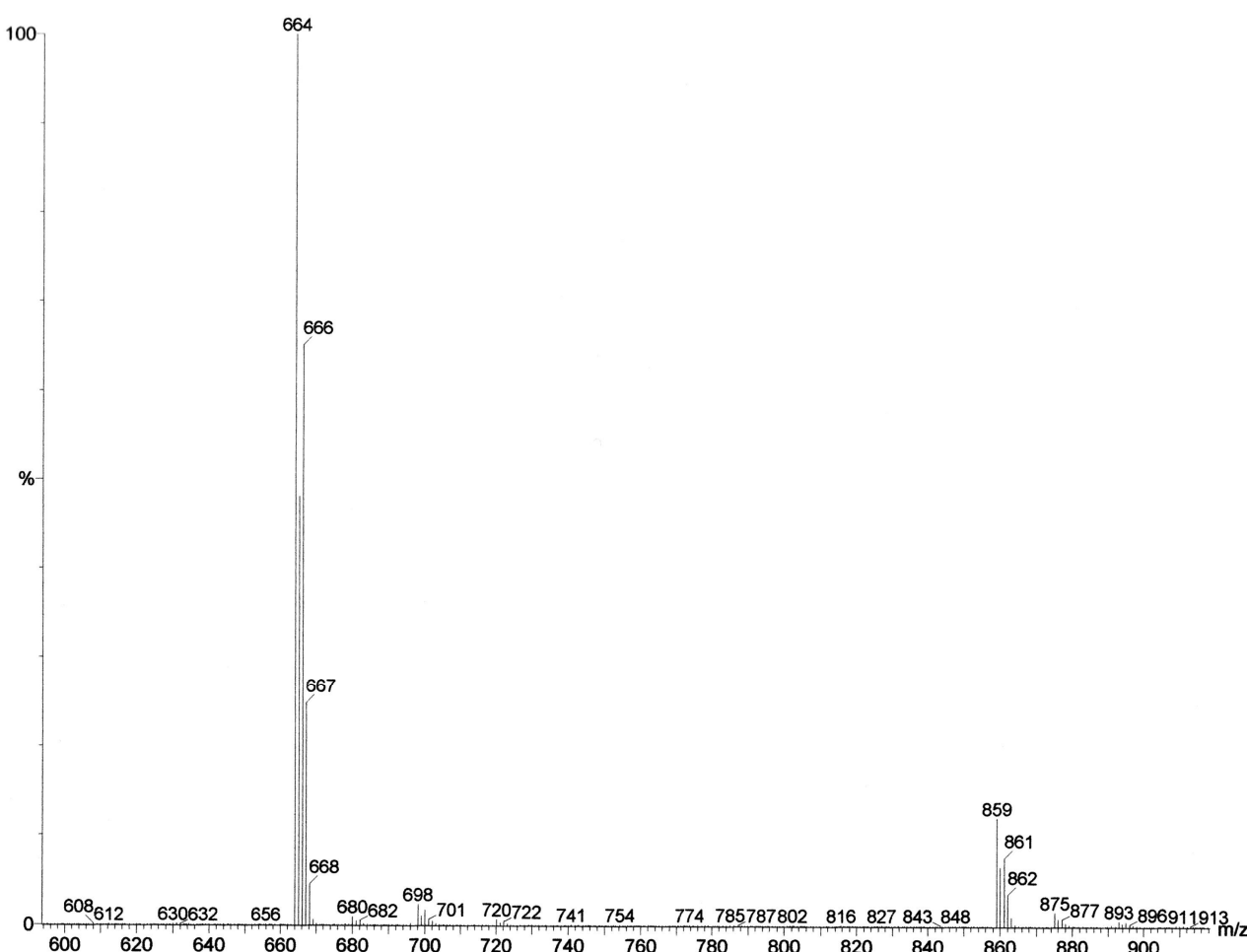


Fig. S1. $[Cu_n(N^N)_n(dppe)_n]^{n+}$ ($n = 1,2$): (top) ESI-MS spectrum (positive ions region) and (down) comparison of the experimental isotopic pattern distribution (left) with those simulated for $[Cu(N^N)(dppe)]^+$ (a) and $[Cu_2(N^N)_2(dppe)]^{2+}$ (b), respectively.

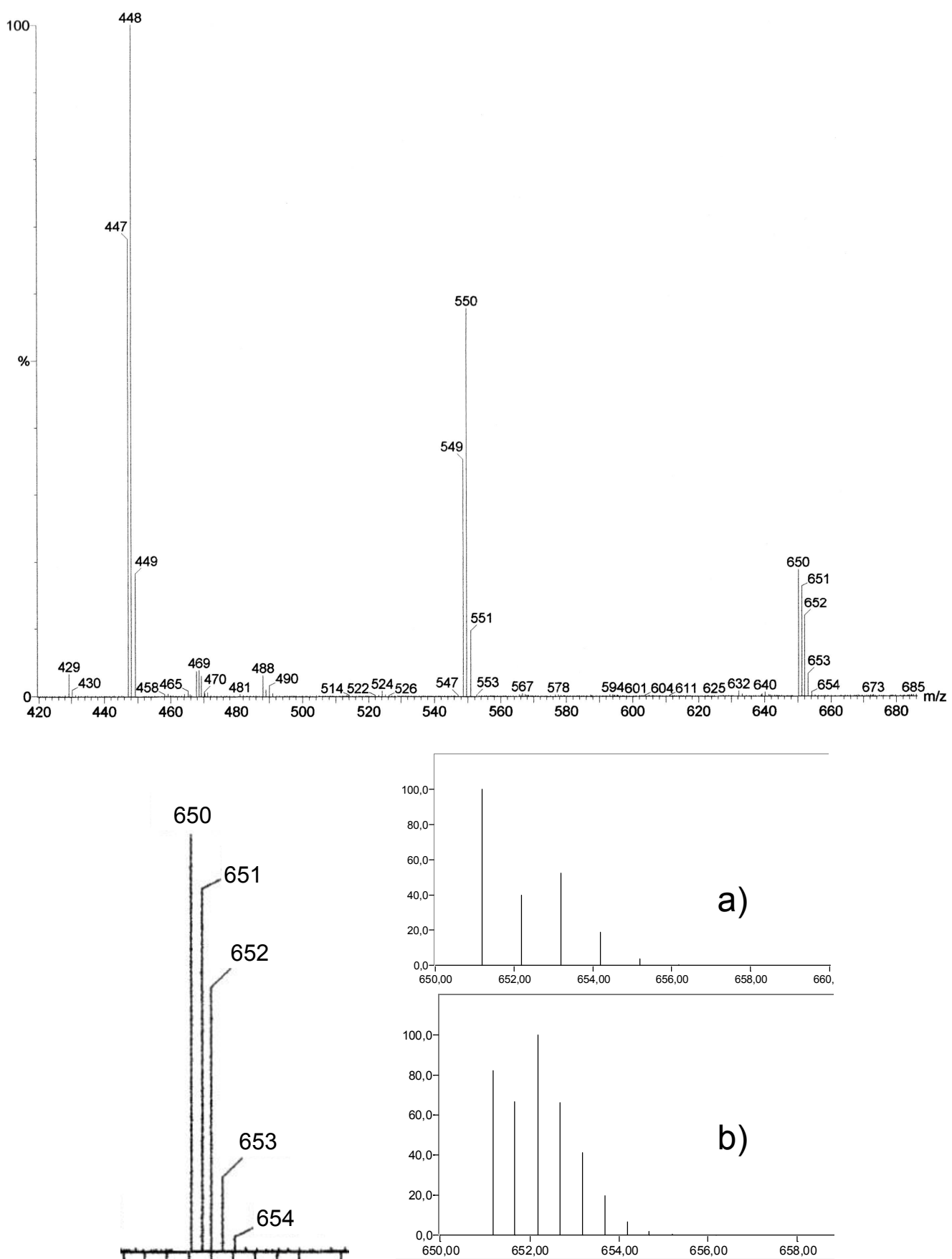


Fig. S2. (top) ESI-MS spectrum (positive ions) of $[Cu_n(N^N)_n(dppm)_n]^{n+}$ ($n = 1,2$) and (down) comparison of the experimental isotopic pattern distribution (left) with those simulated for $[Cu(N^N)(dppm)]^+$ (a) and $[Cu_2(N^N)_2(dppm)_2]^{2+}$ (b), respectively.

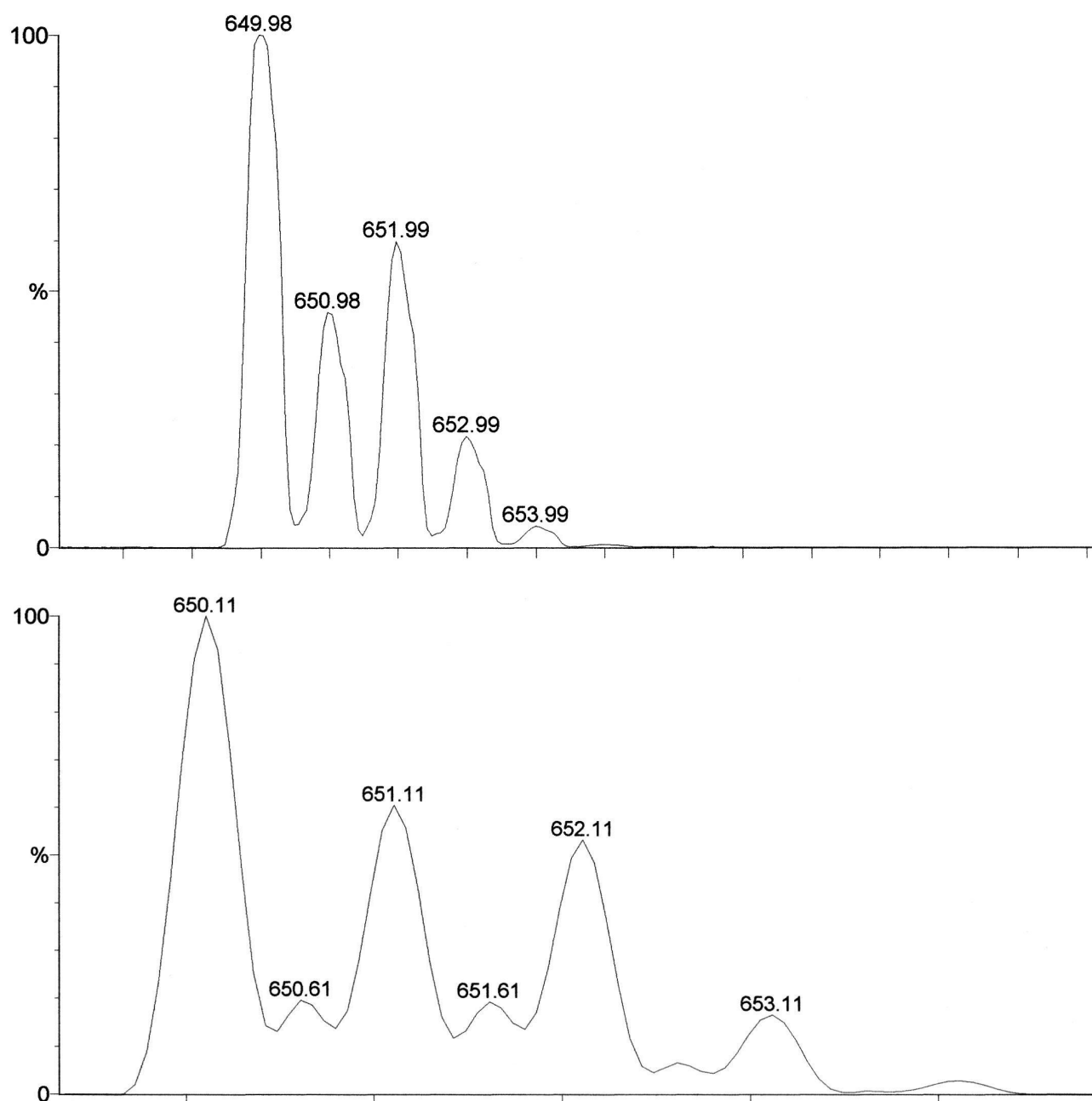


Fig. S3. High Resolution ESI-MS spectra (positive ions) of $[\text{Cu}_n(\text{N}^{\wedge}\text{N})_n(\text{dppm})_n]^{n+}$ ($n = 1,2$) showing the gradual appearance (bottom) of the peaks spaced by $1/2\text{ }m/z$ units that are due to the dinuclear dimeric species $[\text{Cu}_2(\text{N}^{\wedge}\text{N})_2(\text{dppm})_2]^{2+}$.

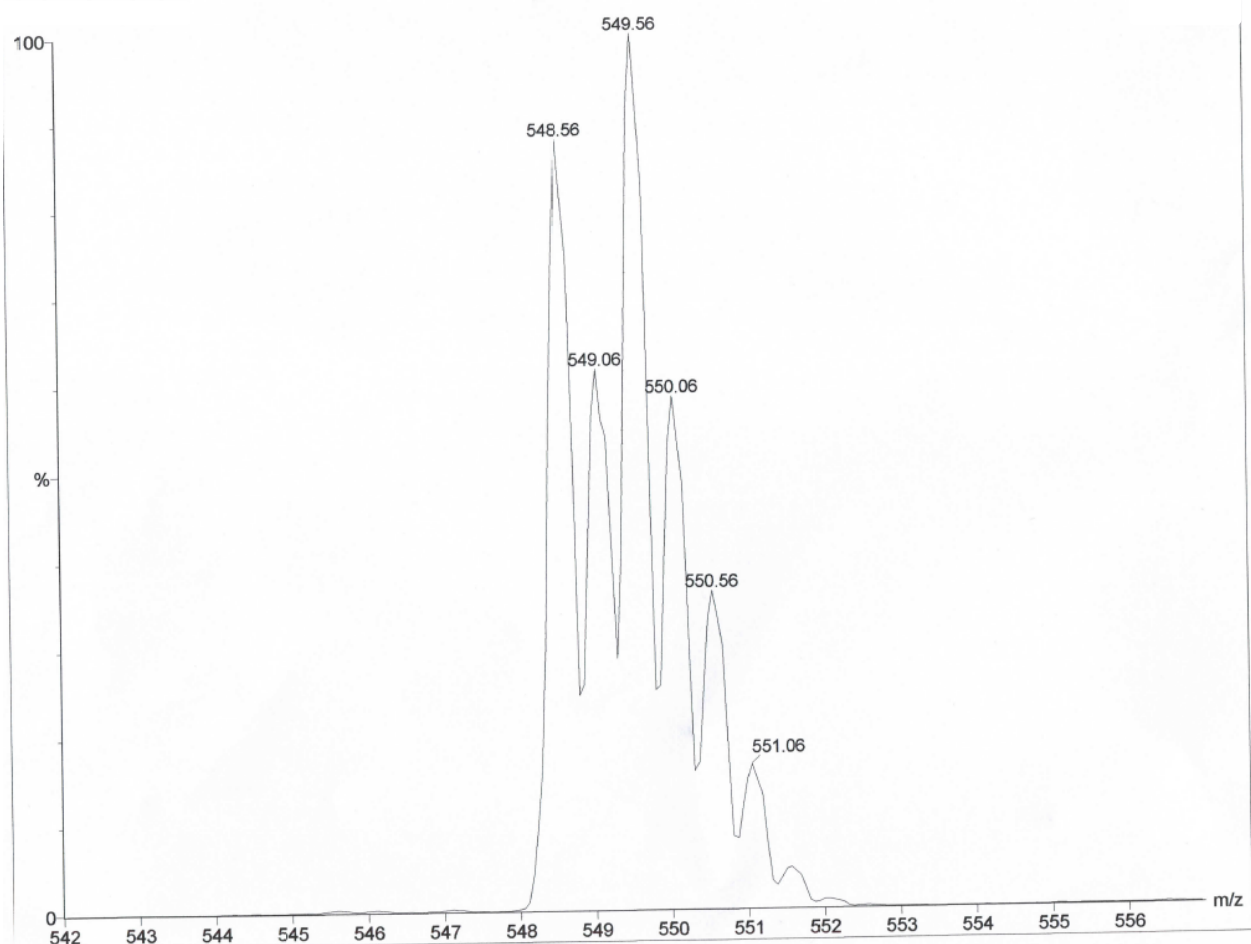


Fig. S4. High Resolution ESI-MS spectra (positive ions) of $[\text{Cu}_n(\text{N}^{\wedge}\text{N})_n(\text{dppm})_n]^{n+}$ ($n = 1,2$) showing the isotopic distribution pattern, with peaks spaced by $1/2 m/z$ units, of the signal centered at $550 m/z$, that is due to bis-cationic dimer $[\text{Cu}_2(\text{N}^{\wedge}\text{N})(\text{dppm})_2]^{2+}$.

NMR (^1H , ^{13}C , ^{31}P) spectra

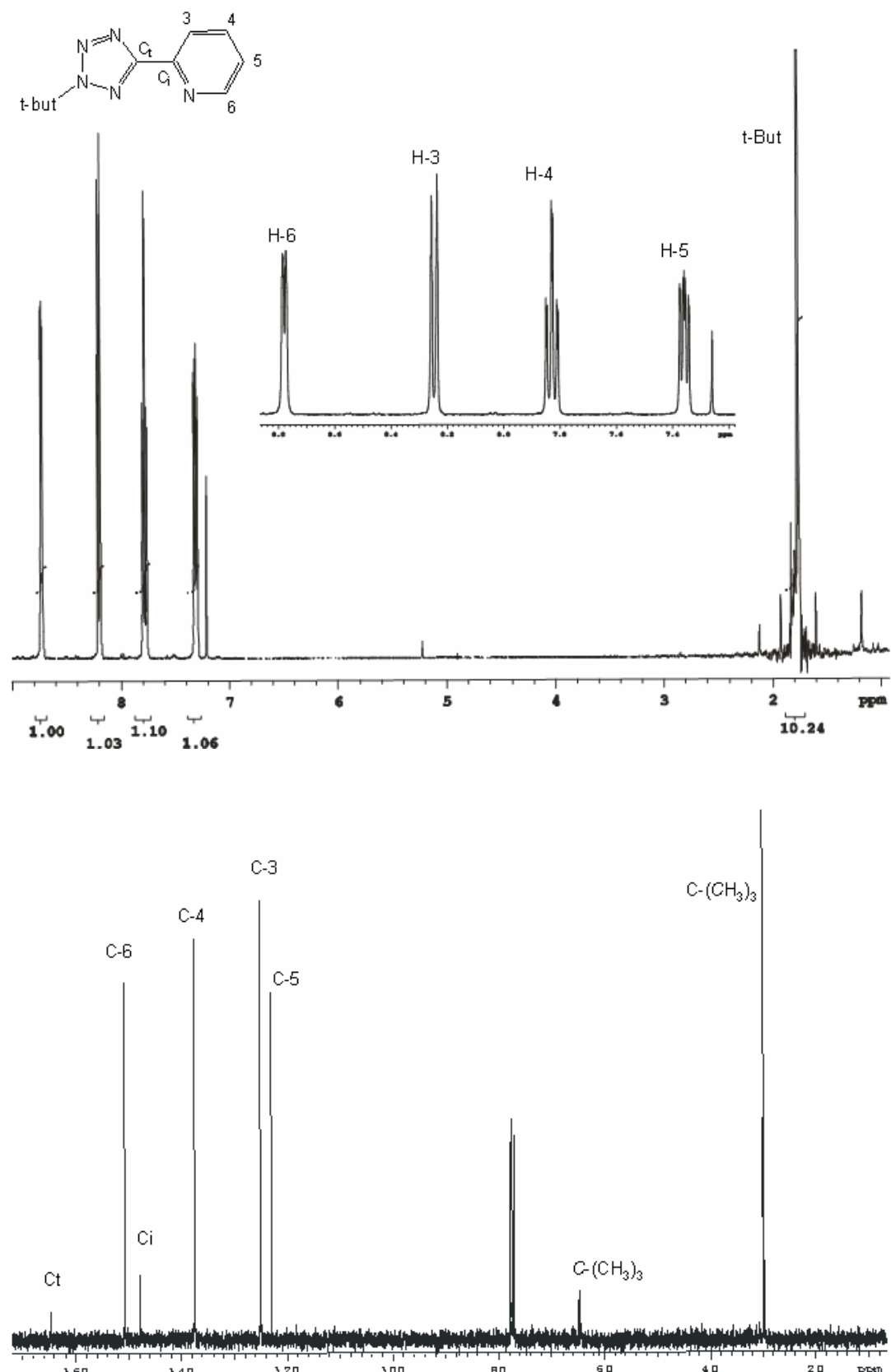


Fig. S5. ${}^1\text{H}$ (CDCl₃, 400 MHz, r.t., top) and ${}^{13}\text{C}$ (CDCl₃, 101 MHz, r.t., bottom) NMR spectra of the free ligand $\text{N}^{\wedge}\text{N}$

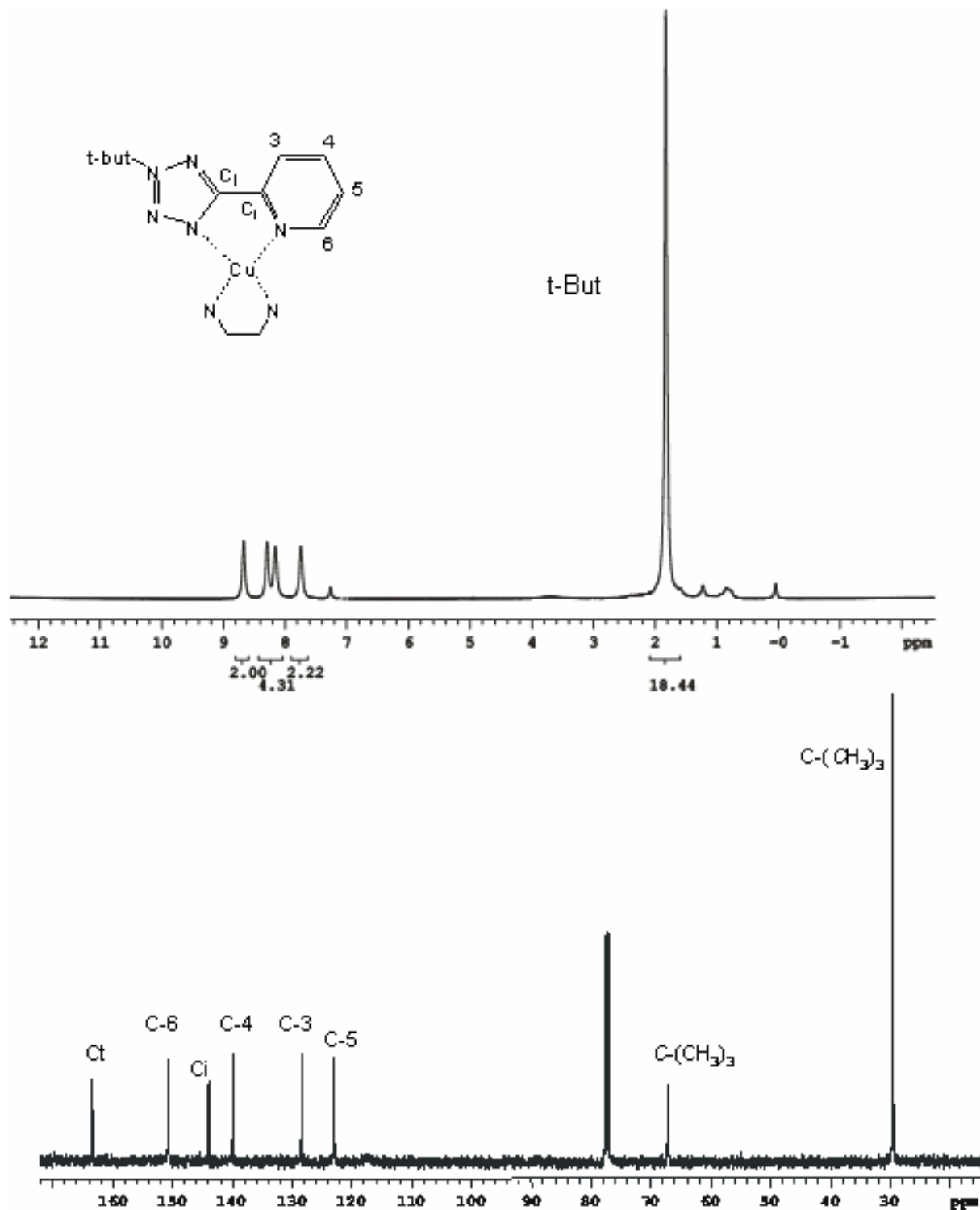


Fig. S6. ^1H NMR (CDCl_3 , 400 MHz, r.t., top) and ^{13}C NMR (CDCl_3 , 101 MHz, r.t., bottom) spectra of the homoleptic complex $[\text{Cu}(\text{N}^{\wedge}\text{N})_2]\text{[BF}_4\text{]}$.

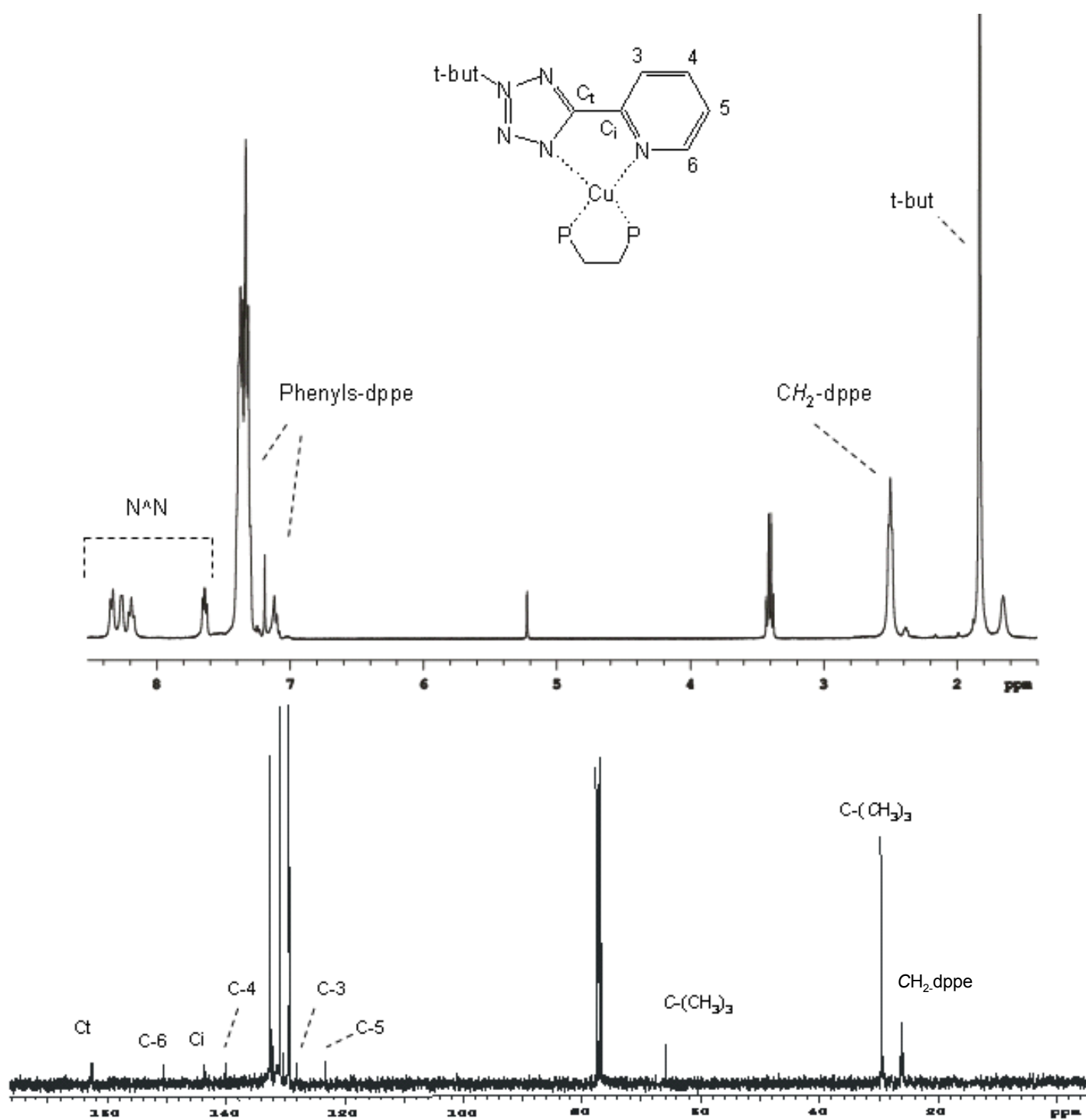


Fig. S7. ^1H NMR (CDCl₃, 400 MHz, r.t., top) and ^{13}C NMR (CDCl₃, 101 MHz, r.t., bottom) spectra of the heteroleptic species considered as [Cu₂(N³⁻N)₂(dppe)₂][BF₄]₂.

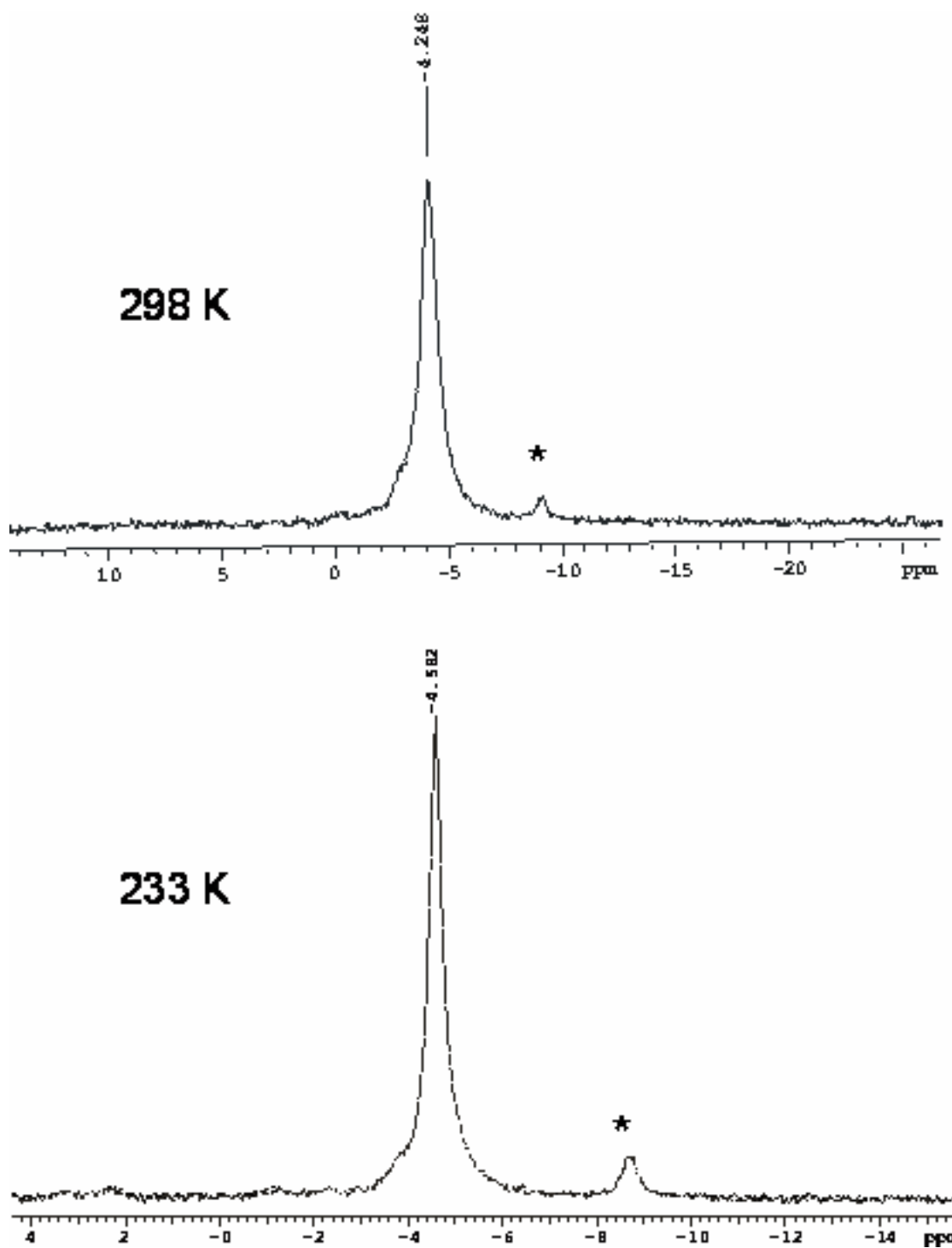


Fig. S8. VT ^{31}P NMR (CDCl_3 , 162 MHz) spectra of the heteroleptic species considered as $[\text{Cu}_2(\text{N}^{\wedge}\text{N})_2(\text{dppe})_2][\text{BF}_4]_2$ recorded at 298 K (top) and 233 K (bottom). The signal marked with an asterisk is relative to small amounts of $[\text{Cu}(\text{dppe})_2][\text{BF}_4]$.

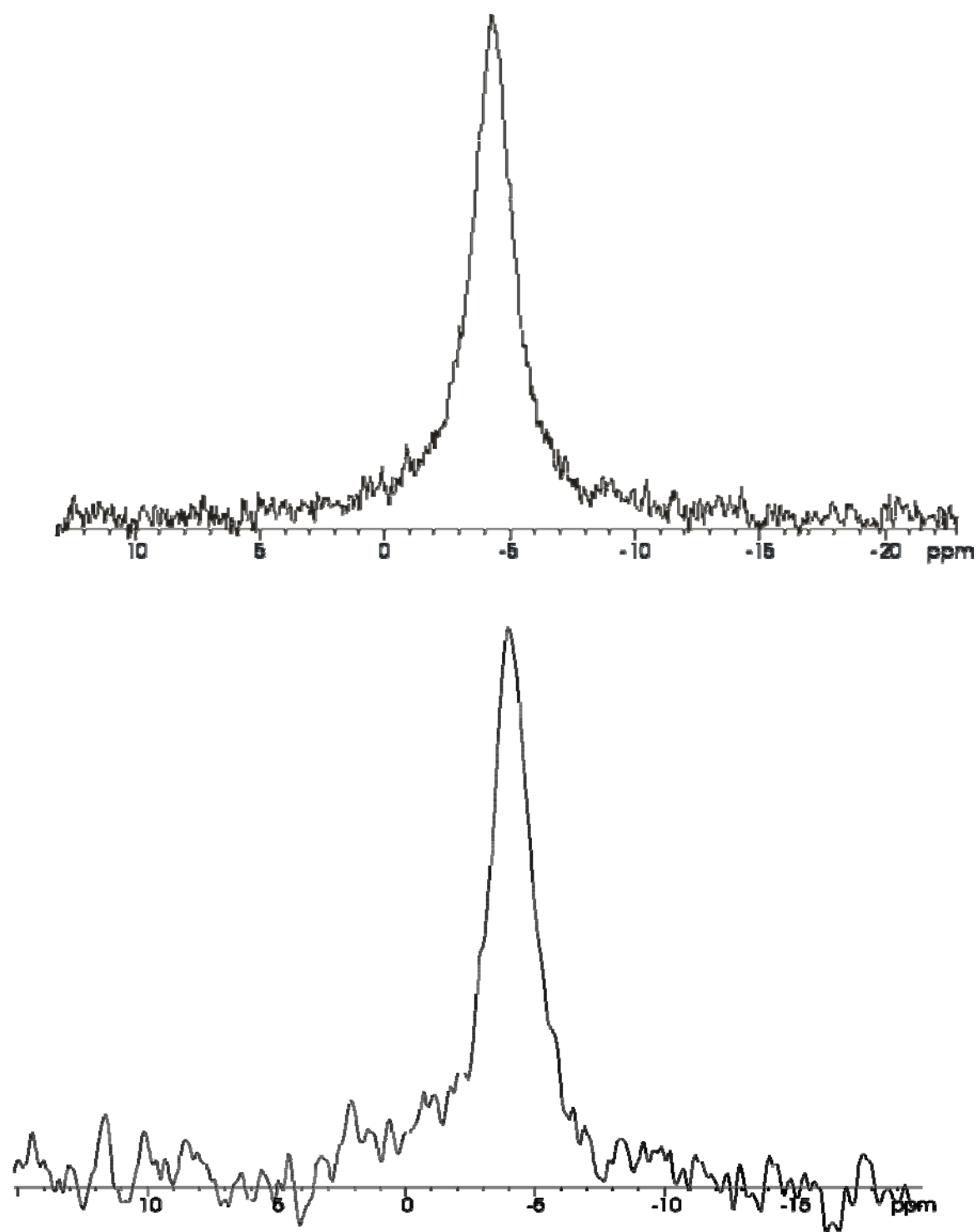


Fig. S9. Stacking plot of ^{31}P NMR spectra (CDCl_3 as the solvent, room temperature) of the complex considered as $[\text{Cu}_2(\text{N}^{\wedge}\text{N})_2(\text{dppe})_2][\text{BF}_4]_2$ at different concentrations: $2.0 \times 10^{-2} \text{ M}$ (top) and $2.0 \times 10^{-4} \text{ M}$ (bottom).

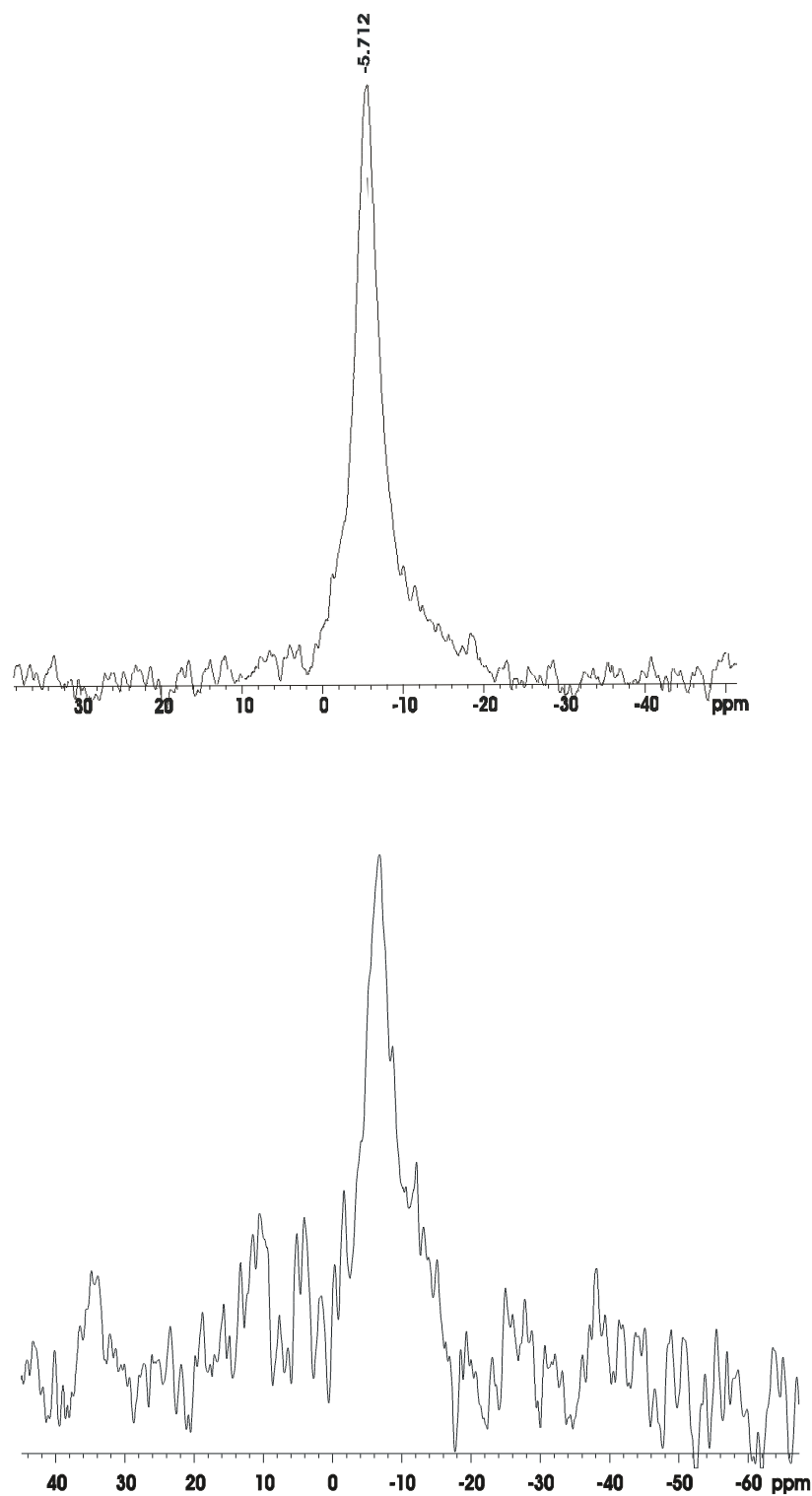


Fig. S10. Stacking plot of ^{31}P NMR spectra (162 MHz, CD_3CN as the solvent, room temperature) of the samples obtained by dissolving solid $[\text{Cu}_2(\text{N}^{\wedge}\text{N})_2(\text{dppe})_2][\text{BF}_4]_2$ in CD_3CN . The spectra refer to samples at different concentrations: $2.0 \times 10^{-2} \text{ M}$ (top) and $2.0 \times 10^{-4} \text{ M}$ (bottom).

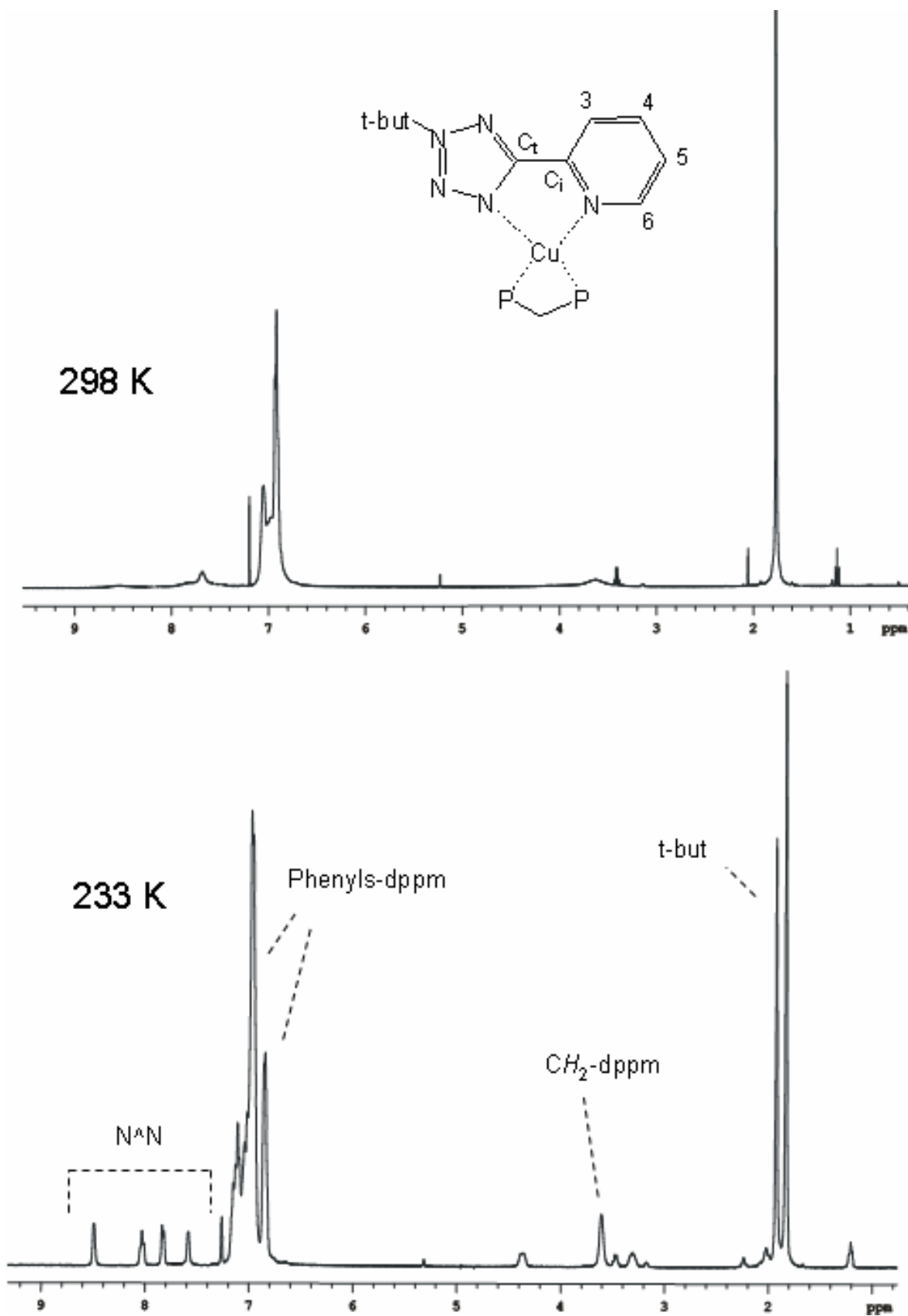


Fig. S11. VT ¹H NMR (CDCl₃, 400 MHz) spectra of the heteroleptic species considered as a mixture of [Cu(N^{^N})₂(dppm)₂][BF₄]₂ and [Cu(N^{^N})(dppm)][BF₄] recorded at 298 K (top) and 233 K (bottom).

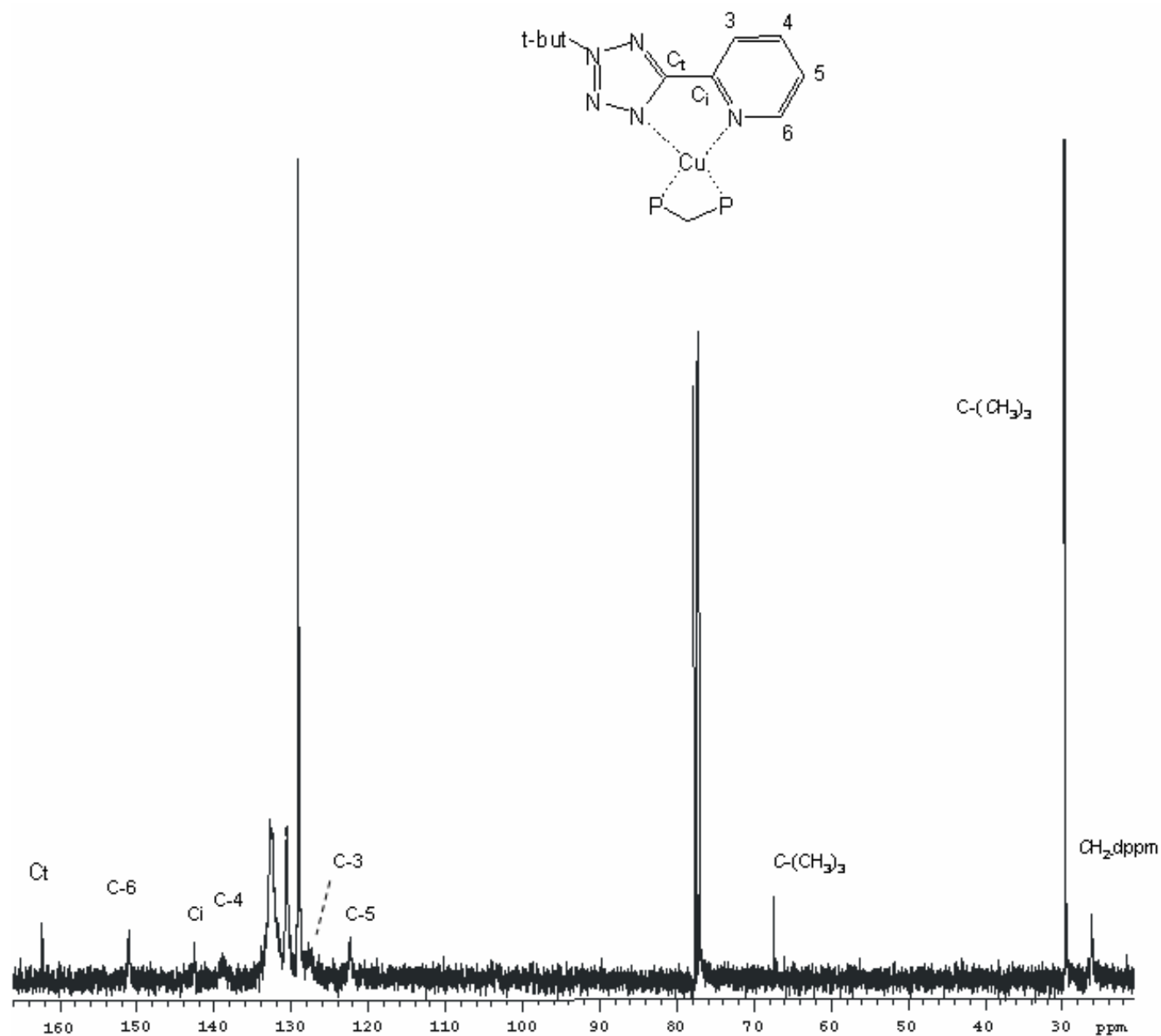


Fig. S12. ^{13}C NMR (CDCl_3 , 101 MHz, r.t.) spectrum of the heteroleptic species considered as a mixture of $[\text{Cu}_2(\text{N}^{\wedge}\text{N})_2(\text{dppm})_2][\text{BF}_4]_2$ and $[\text{Cu}(\text{N}^{\wedge}\text{N})(\text{dppm})][\text{BF}_4]$.

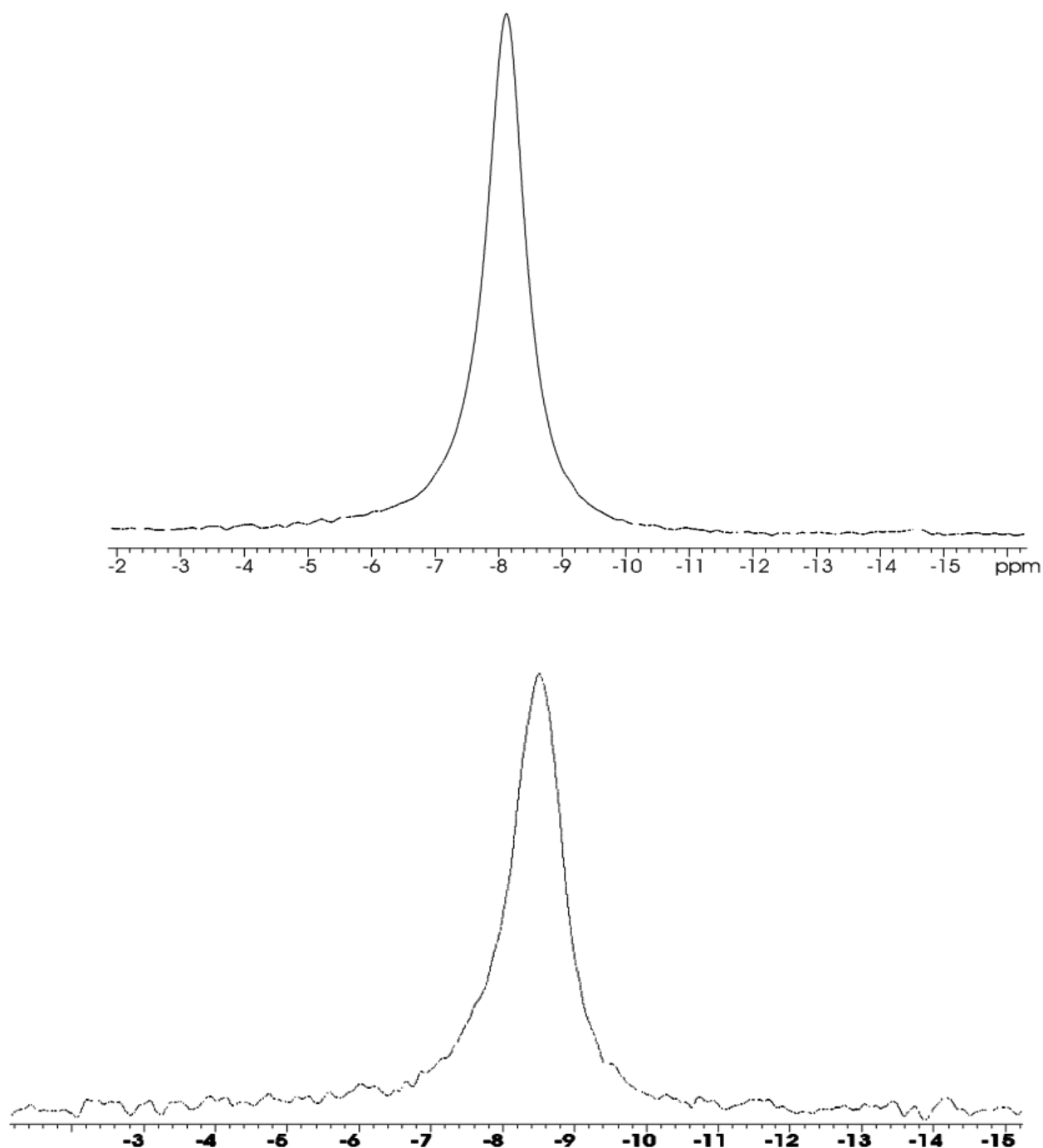


Fig. S13. Stacking plot of ^{31}P NMR spectra (CD_3CN as the solvent, room temperature) of the complex considered as the mixture of monomeric ($n=1$) and dimeric ($n=2$) $[\text{Cu}_n(\text{N}^{\wedge}\text{N})_n(\text{dppm})_n][\text{BF}_4]_n$ at different concentrations: $2.0 \times 10^{-2} \text{ M}$ (top) and $2.0 \times 10^{-4} \text{ M}$ (bottom).

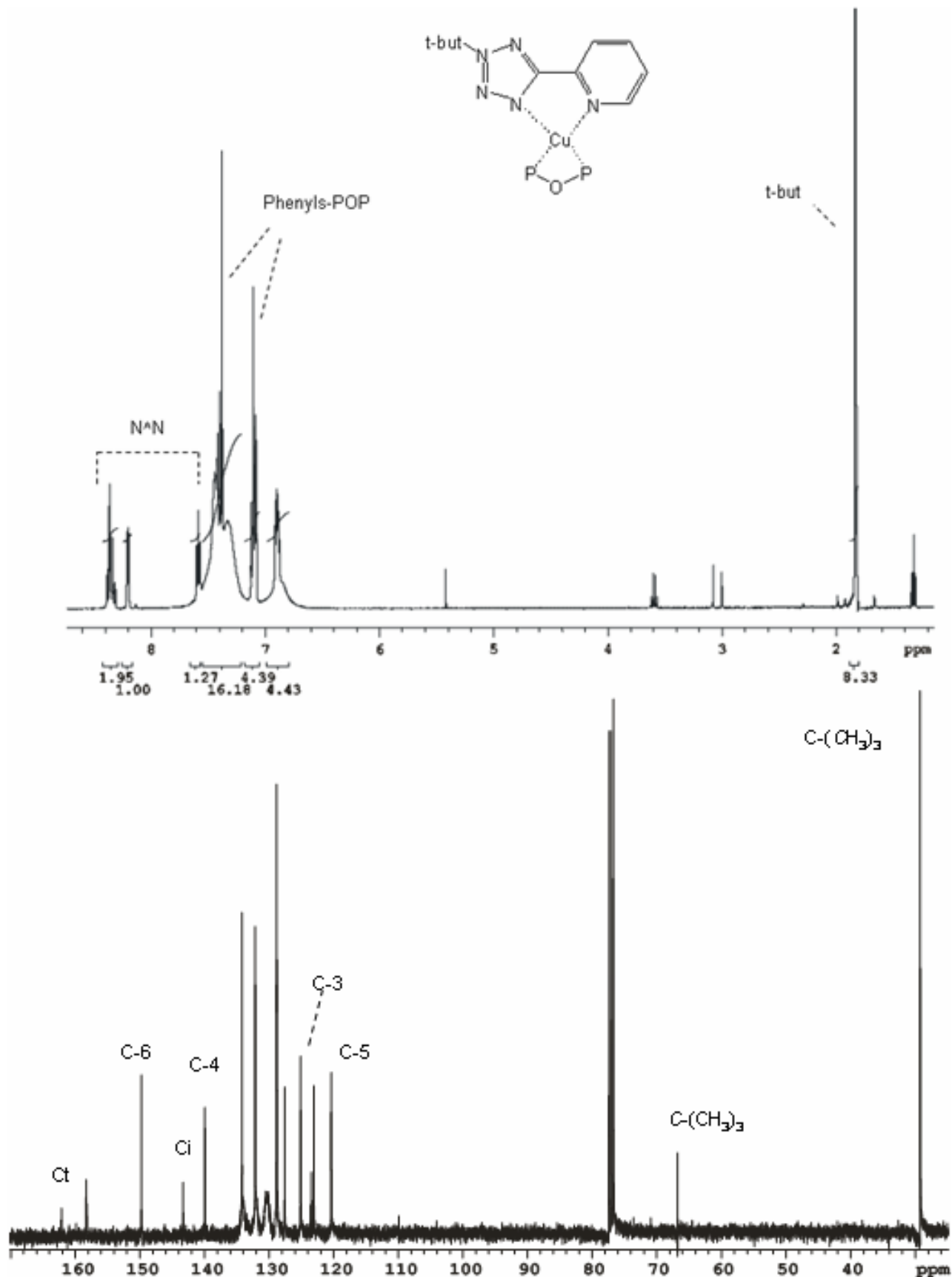


Fig. S14. H NMR (CDCl₃, 400 MHz, r.t., top) and ^{13}C NMR (CDCl₃, 101 MHz, r.t., bottom) spectra of the heteroleptic species considered as [Cu(N⁺N)(POP)][BF₄].

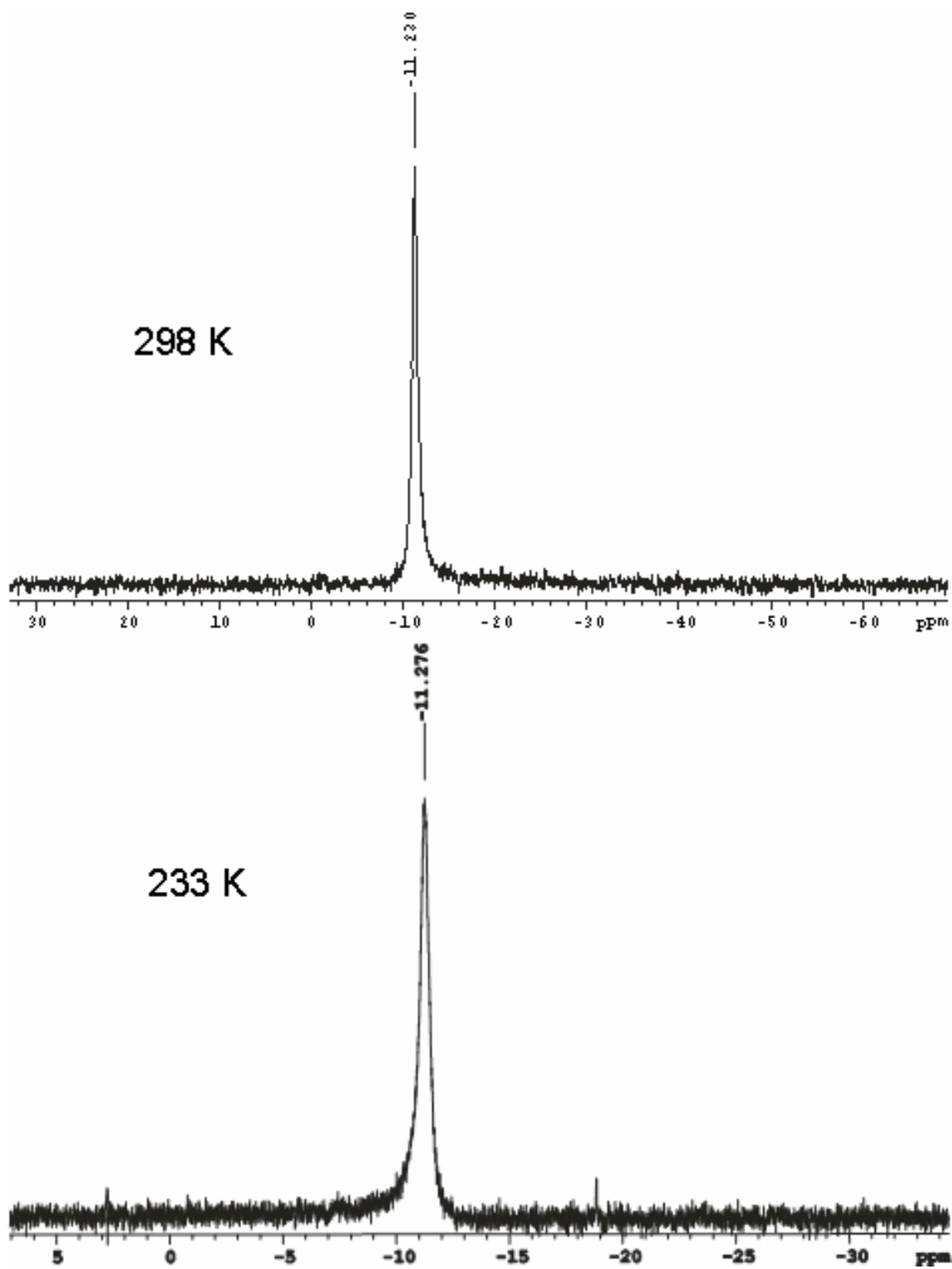


Fig. S15. VT ^{31}P NMR (CDCl_3 , 162 MHz) spectra of the heteroleptic species considered as $[\text{Cu}(\text{N}^{\wedge}\text{N})(\text{POP})][\text{BF}_4]$ recorded at 298 K (top) and 233 K (bottom).